

## RESEARCH ARTICLE

# Tissue-type plasminogen activator regulates p35-mediated Cdk5 activation in the postsynaptic terminal

Ariel Diaz<sup>1,\*</sup>, Valerie Jeanneret<sup>2,\*</sup>, Paola Merino<sup>1</sup>, Patrick McCann<sup>1</sup> and Manuel Yepes<sup>1,2,3,‡</sup>

## ABSTRACT

Neuronal depolarization induces the synaptic release of tissue-type plasminogen activator (tPA). Cyclin-dependent kinase-5 (Cdk5) is a member of the family of cyclin-dependent kinases that regulates cell migration and synaptic function in postmitotic neurons. Cdk5 is activated by its binding to p35 (also known as Cdk5r1), a membrane-anchored protein that is rapidly degraded by the proteasome. Here, we show that tPA prevents the degradation of p35 in the synapse by a plasminogen-dependent mechanism that requires open synaptic N-methyl-D-aspartate (NMDA) receptors. We show that tPA treatment increases the abundance of p35 and its binding to Cdk5 in the postsynaptic density (PSD). Furthermore, our data indicate that tPA-induced p35-mediated Cdk5 activation does not induce cell death, but instead prevents NMDA-induced ubiquitylation of postsynaptic density protein-95 (PSD-95; also known as Dlg4) and the removal of GluR1 (also known as Gria1)-containing  $\alpha$ -amino-3-hydroxy-5-methyl-4-isoxazolepropionic acid (AMPA) receptors from the PSD. These results show that the interaction between tPA and synaptic NMDA receptors regulates the expression of AMPA receptor subunits in the PSD via p35-mediated Cdk5 activation. This is a novel role for tPA as a regulator of Cdk5 activation in cerebral cortical neurons.

**KEY WORDS:** Tissue-type plasminogen activator, Plasmin, Cyclin-dependent kinase-5, NMDA receptors, Postsynaptic density

## INTRODUCTION

Tissue-type plasminogen activator (tPA) is a serine proteinase that in the central nervous system (CNS) is found not only in the intravascular space, where it catalyzes the conversion of plasminogen into plasmin, but also in glial cells and neurons, where its function has been the focus of intense research over the past two decades (Yepes et al., 2009). Indeed, the discovery in the murine brain of tPA-catalyzed proteolysis in the hippocampus, hypothalamus, amygdala, thalamus and cerebellum (Sappino et al., 1993) was rapidly followed by the finding that neurons are a major source of tPA synthesis *in vivo*, and that tPA plays a central role in the regulation of synaptic plasticity (Qian et al., 1993) via plasmin-dependent and -independent activation of various cell signaling pathways.

TPA is stored in the presynaptic vesicles of cerebral cortical neurons, and its release at extrasynaptic sites activates the synaptic vesicle cycle (Wu et al., 2015; Yepes et al., 2016), and promotes

functional and structural changes in the synapse required for the development of long-term potentiation (Qian et al., 1993), learning (Seeds et al., 1995), stress-induced anxiety (Pawlak et al., 2003) and visual cortex plasticity (Müller and Griesinger, 1998). Interestingly, recent studies indicate that the release of tPA into the synaptic cleft also modulates the response of the postsynaptic terminal to the presynaptic release of glutamate (Jeanneret et al., 2016), and has a direct effect on the structure and receptor composition of the postsynaptic density (PSD) (Jeanneret et al., 2018).

Cyclin-dependent kinase-5 (Cdk5) is a member of the family of cyclin-dependent kinases found in postmitotic neurons (Dhavan and Tsai, 2001). Cdk5 regulates neuronal migration (Dhavan and Tsai, 2001), the presynaptic release of neurotransmitters (Matsubara et al., 1996) and synaptic vesicle endocytosis (Floyd et al., 2001). These findings have led to this kinase being considered as a master regulator of synaptic function (Dhavan and Tsai, 2001) and, in line with these observations, its dysregulation has been associated with neuronal death and neurodegeneration (Fischer et al., 2005). Cdk5 is activated by its binding to specific proteins, p35 (also known as Cdk5r1) and p39 (also known as Cdk5r2), and their corresponding cleaved products p25 and p29 (Shah and Lahiri, 2014). p35 is a membrane-anchored protein assembled by a carboxyl terminal with a p25 component and a N-terminus with a p10 region (Tang et al., 1997). p35 is regulated transcriptionally by multiple factors, including nerve growth factor (NGF), brain-derived neurotrophic factor (BDNF) and tumor necrosis factor- $\alpha$  (TNF $\alpha$ ) (Harada et al., 2001; Utreras et al., 2009); and postranscriptionally by several microRNAs (Moncini et al., 2017). Furthermore, its degradation is mediated by ubiquitin-dependent and -independent pathways (Takasugi et al., 2016).

The PSD is an electron-dense structure of excitatory synapses that anchors signaling molecules and receptors to the postsynaptic membrane (Ziff, 1997). Postsynaptic density protein-95 (PSD-95; also known as Dlg4) is the most abundant scaffolding protein in the PSD (Cheng et al., 2006), and its ability to interact with membrane receptors, cytoskeletal proteins, ion channels and intracellular proteins via its PSD-95/Disks large (Dlg)/zona occludens-1 (ZO-1) (PDZ) domains, bestows on this protein a unique role as a molecular organizer and regulator of synaptic function (Tomita et al., 2001). tPA has a direct effect on the abundance of PSD-95 in the PSD (Jeanneret et al., 2018, 2016), and Cdk5 phosphorylates (Morabito et al., 2004) and regulates the ubiquitylation and proteasomal degradation of PSD-95 (Bianchetta et al., 2011). However, it is still unknown whether there is a functional association between Cdk5 and tPA in cerebral cortical neurons.

Our data indicate that tPA prevents the degradation of p35 in the synapse by a mechanism that requires open synaptic N-methyl-D-aspartate (NMDA) receptors. We found that the increased abundance of p35 induced by tPA leads to it binding to Cdk5 in the PSD, and that tPA-induced p35-mediated Cdk5 activation prevents NMDA-induced ubiquitylation of PSD-95 and the removal

<sup>1</sup>Division of Neuropharmacology and Neurologic Diseases, Yerkes National Primate Research Center, Atlanta, GA 30329, USA. <sup>2</sup>Department of Neurology, Emory University School of Medicine, Atlanta, GA 30322, USA. <sup>3</sup>Department of Neurology, Veterans Affairs Medical Center, Atlanta, GA 30033, USA.

\*These authors contributed equally to this work

‡Author for correspondence (myepes@emory.edu)

© M.Y., 0000-0002-5224-9663

of GluR1 (also known as Gria1)-containing  $\alpha$ -amino-3-hydroxy-5-methyl-4-isoxazolepropionic acid (AMPA) receptors from the PSD. In summary, the results presented here show that the interaction between tPA and synaptic NMDA receptors regulates the expression of AMPA receptor subunits in the PSD via p35-mediated Cdk5 activation. This is a novel role for tPA as a regulator of Cdk5 activation in cerebral cortical neurons.

## RESULTS

### tPA increases the abundance of p35 in the PSD of cerebral cortical neurons

Because our early studies indicate that tPA increases the thickness of the PSD via Cdk5 activation (Jeanneret et al., 2016), we decided to study the expression of p35, a specific Cdk5 activator (Shah and Lahiri, 2014), in extracts prepared from wild-type (Wt) cerebral cortical neurons treated for 0–60 s with either 5 nM proteolytically active or inactive tPA, or 100 nM plasmin. We found that tPA induces a rapid increase in the abundance of p35 (Fig. 1A,B) by a mechanism that requires its proteolytic activity (Fig. 1C,D). In agreement with these observations, we also detected an increase in

the abundance of p35 in neurons treated with plasmin (Fig. 1E,F). Because p35 has a short half-life (Patrick et al., 1998), and its abundance in the synapse is controlled mainly by ubiquitin-dependent and -independent degradation pathways (Takasugi et al., 2016), and to a lesser extent by local protein synthesis (Patrick et al., 1998; Shah and Lahiri, 2014), we postulated that the rapid effect of tPA on p35 expression is due to inhibition of its degradation. To test this hypothesis, we first studied the effect of protein synthesis inhibition on the abundance of p35. Our data indicate that the expression of p35 decreases below baseline levels following 30 min of treatment with puromycin, when protein synthesis has been inhibited and the degradation of membrane-bound p35 has already taken place [the half-life of p35 is <20 min (Patrick et al., 1998)]. We then studied the expression of p35 in neurons treated for 15 s with 5 nM tPA (to prevent the degradation of membrane-bound p35) followed by 30 min of incubation with puromycin. We found that p35 expression in cells pretreated with tPA was higher than in those pretreated with vehicle (control; Fig. 1G,H). To further investigate the possibility that tPA inhibits the degradation of p35, we studied its expression in Wt cerebral cortical neurons incubated

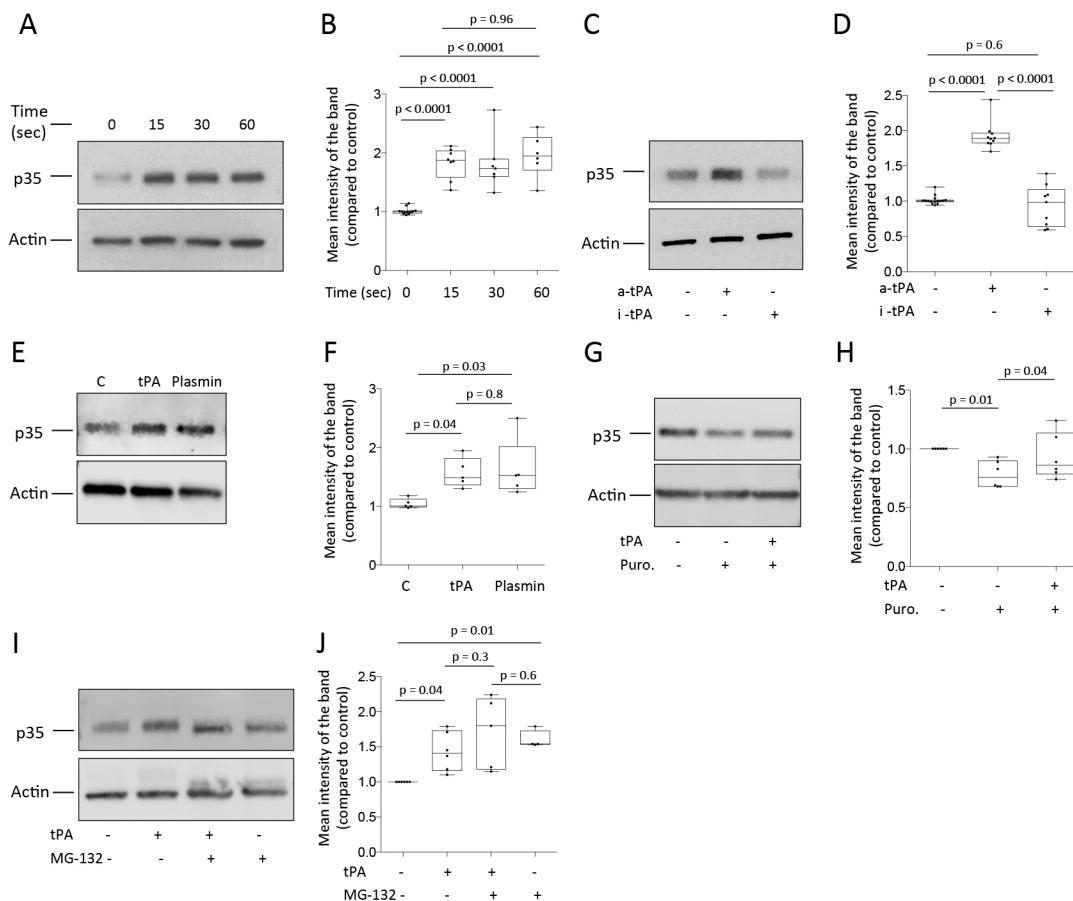


**Fig. 1. Effect of tPA on p35 expression in cerebral cortical neurons.** (A–F) Representative western blot analyses (A,C,E) and quantification of the mean intensity of the band (B,D,F) of p35 expression in whole-cell extracts prepared from Wt cerebral cortical neurons incubated for 0–60 s with 5 nM tPA (A,B), or for 60 s with 5 nM proteolytically active tPA (a-tPA) or inactive tPA (i-tPA) (C,D), or for 60 s with either 5 nM tPA or 100 nM plasmin (E,F).  $n=13$  (time 0), 8 (time 15 s), 7 (time 30 s) and 6 (time 60 s) observations in B; 15 (control), 10 (active tPA) and 9 (inactive tPA) observations in D; and 5 observations per experimental condition in F. Statistical analysis in B, D and F: one-way ANOVA with Tukey's correction in B and D, and with Dunnett's correction in F. (G,H) Representative western blot analyses (G) and quantification of the mean intensity of the band (H) of p35 expression in whole-cell extracts prepared from Wt cerebral cortical neurons treated for 15 s with 5 nM tPA or a comparable volume of vehicle (control), and then incubated for 30 min with 270  $\mu$ M puromycin.  $n=6$  observations per experimental group. Statistical analysis: one-way ANOVA with Tukey's correction. (I,J) Representative western blot analysis (I) and quantification of the mean intensity of the band (J) of p35 expression in Wt cerebral cortical neurons incubated for 15 s with tPA, alone or in the presence of 100  $\mu$ M MG-132, or with MG-132 alone.  $n=6$  per experimental group. Statistical analysis: two-way ANOVA with Holm–Sidak's correction. For the box plots, the box represents the 25–75th percentiles, and the median is indicated. The whiskers show the complete range. Each dot represents values for individual observations.

for 15 s with tPA, alone or in the presence of 100  $\mu$ M MG-132, a proteasomal inhibitor, or with MG-132 alone. We found that tPA or MG-132 alone, or a combination of tPA and MG-132, increases the abundance of p35 to comparable levels (Fig. 1I,J).

To further characterize these observations, we studied the expression of p35 in microtubule associated protein-2 (MAP-2)- and Tau (also known as Mapt)-positive extensions (to delineate dendrites and axons, respectively) from Wt cerebral cortical neurons incubated for 60 s with 5 nM tPA or a comparable volume of vehicle (control). Our data indicate that tPA increases the expression of p35 in dendrites (Fig. 2A–C) but not axons (Fig. 2D–F). To investigate whether tPA increases the abundance of p35 in the synapse or in the shaft of neuronal extensions, we studied the expression of p35 in extracts from synaptoneurosomes prepared from Wt cerebral cortical neurons incubated for 0–60 s with 5 nM tPA or a comparable volume of vehicle (control). Our results show that tPA increases the abundance of p35 in the synapse (Fig. 2G,H). To determine whether the effect of tPA on p35 occurs in the pre- or

postsynaptic terminal (synaptosomes are assembled by the sealed presynaptic bouton and the attached postsynaptic terminal), we quantified the number of p35/PSD-95 (detects p35 in the postsynaptic terminal)- and p35/bassoon (identifies p35 in the presynaptic terminal)-positive puncta in Wt neurons treated for 60 s with 5 nM tPA or vehicle (control). We found that the number of p35/PSD-95-positive puncta per 50  $\mu$ m increases from  $9 \pm 1.48$  in control cells to  $25.55 \pm 2.5$  in tPA-treated neurons (Fig. 2I,J;  $n=80$  dendrites from ten Wt neurons per experimental group;  $P < 0.0001$ ; two-tailed Student's *t*-test). In contrast, tPA did not have an effect on the number of p35/bassoon-positive puncta (Fig. 2K,L). Because NMDA receptors mediate several effects of tPA in the PSD (Nicole et al., 2001; Samson et al., 2008), we then studied the expression of p35 in PSD extracts prepared from Wt cerebral cortical neurons treated with tPA, alone or in the presence of 10  $\mu$ M of MK-801. Our data corroborate our observation that tPA increases the abundance of p35 in the PSD, and indicate that this effect requires open synaptic NMDA receptors (Fig. 2M,N).

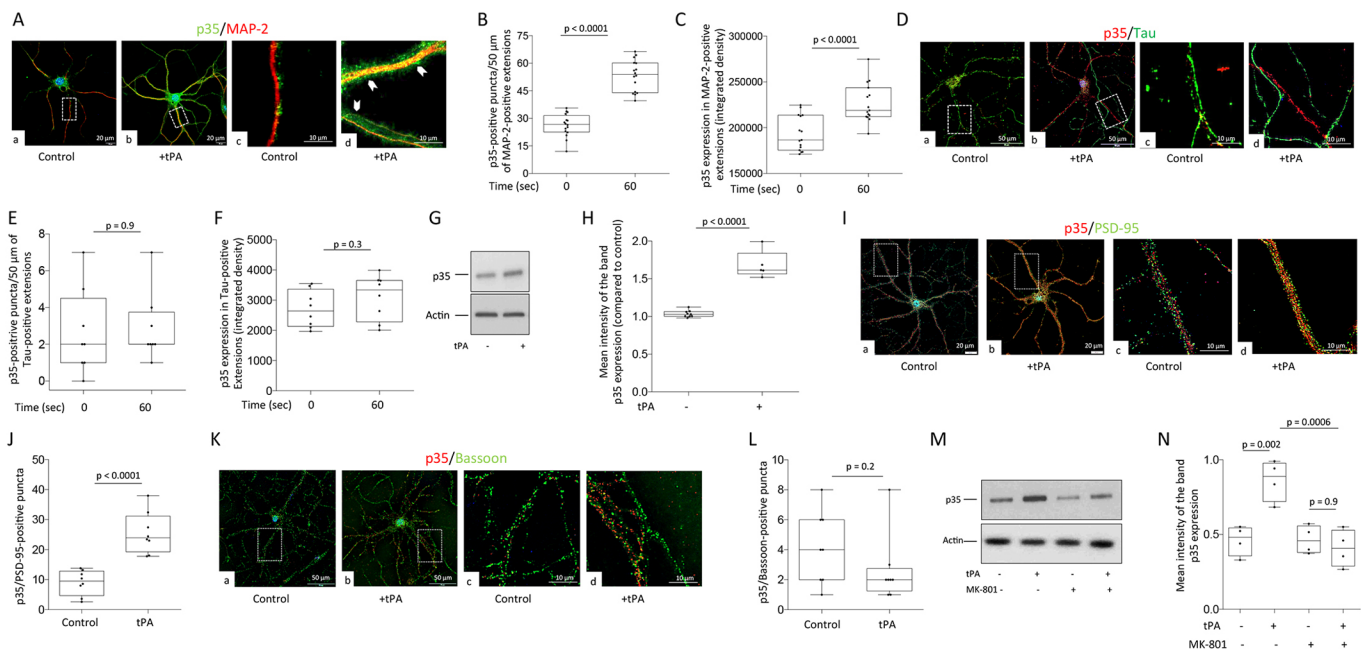


**Fig. 2. Synaptic NMDA receptors mediate the effect of tPA on the expression of p35 in the PSD of cerebral cortical neurons.** (A) Representative confocal microscopy micrographs (60 $\times$  magnification) of p35 (green) and MAP-2 (red) expression in Wt cerebral cortical neurons incubated for 60 s with vehicle (control; a, c) or 5 nM tPA (b, d). c and d correspond to a 4 $\times$  electronic magnification from the areas demarcated by the dashed line boxes in a and b, respectively. Arrowheads in d indicate p35-positive dendritic spines. (B,C) Mean number of p35-positive puncta per 50  $\mu$ m (B) and integrated density of p35 expression (C) in MAP-2-positive extensions of Wt cerebral cortical neurons incubated for 0–60 s with 5 nM tPA.  $n=80$  MAP-2-positive extensions examined from 16 neurons per experimental group. Threshold: 65–255 for green channel. Statistical analysis: two-tailed Student's *t*-test. (D) Representative confocal microscopy pictures (60 $\times$  magnification) of p35 (red) and Tau (green) expression in Wt cerebral cortical neurons incubated for 60 s with vehicle (control; a, c) or 5 nM tPA (b, d). c and d correspond to a 4 $\times$  electronic magnification from the areas demarcated by the dashed line boxes in a and b, respectively. (E,F) Mean number of p35-positive puncta per 50  $\mu$ m (E) and integrated density of p35 expression (F) in Tau-positive extensions of Wt cerebral cortical neurons incubated for 0–60 s with 5 nM tPA.  $n=40$  Tau-positive extensions examined from eight neurons per experimental group. Threshold: 65–255 for red channel. Statistical analysis: two-tailed Student's *t*-test. (G,H) Representative western blot analysis (G) and quantification of the mean intensity of the band (H) of p35 expression in extracts from synaptoneurosomes prepared from Wt cerebral cortical neurons incubated with vehicle (control;  $n=9$ ) or 5 nM tPA ( $n=5$ ). Statistical analysis: Student's *t*-test. (I) Representative 60 $\times$  confocal microscopy pictures of p35/PSD-95 co-localization in Wt cerebral cortical neurons incubated for 60 s with vehicle (control; a, c) or 5 nM tPA (b, d). c and d correspond to a 4 $\times$  electronic magnification of the areas demarcated by the dashed line boxes in a and b, respectively. (J) Mean number of p35/PSD-95-positive puncta in 80 dendrites examined from ten Wt neurons from eight different coverslips incubated for 60 s with vehicle (control) or 5 nM tPA. Statistical analysis: two-tailed Student's *t*-test. Threshold: 65–255 for red channel and 45–255 for green channel. (K) Representative 60 $\times$  confocal microscopy pictures of p35/bassoon co-localization in Wt cerebral cortical neurons incubated for 60 s with vehicle (control; a, c) or 5 nM tPA (b, d). c and d correspond to a 4 $\times$  electronic magnification of the areas demarcated by the dashed line boxes in a and b, respectively. (L) Mean number of p35/bassoon-positive puncta in 80 dendrites from eight Wt neurons from ten different coverslips incubated for 60 s with vehicle (control) or 5 nM tPA. Statistical analysis: two-tailed Student's *t*-test. Threshold: 65–255 for red channel and 45–255 for green channel. (M,N) Representative western blot analysis (M) and mean intensity of the band (N) of p35 expression in PSD extracts prepared from Wt cerebral cortical neurons incubated for 60 s with 5 nM tPA, alone or in the presence of 20  $\mu$ M MK-801.  $n=4$  observations per group. Statistical analysis: two-way ANOVA with Tukey's correction. For the box plots, the box represents the 25–75th percentiles, and the median is indicated. The whiskers show the complete range. Each dot represents values for individual observations.

### tPA induces p35-mediated Cdk5 activation

Because p35 binding to Cdk5 leads to Cdk5 activation (Shah and Lahiri, 2014), we then used confocal microscopy to study p35/Cdk5 co-localization in dendrites of Wt cerebral cortical neurons incubated for 60 s with 5 nM tPA or vehicle (control). Our data indicate that the number of p35/Cdk5-positive puncta per 50  $\mu\text{m}$  increases from  $99 \pm 11.8$  in control cells to  $172 \pm 21$  in tPA-treated neurons (Fig. 3A,B;  $n=30$  cells per experimental group;  $P=0.005$ ; two-tailed Student's *t*-test). To further corroborate these findings, extracts from tPA- and vehicle (control)-treated neurons were immunoprecipitated with an anti-p35 antibody and immunoblotted with an antibody against Cdk5. We found that treatment with tPA induces not only the expression of p35 but also its binding to Cdk5 (Fig. 3C,D). Because it has been postulated that Cdk5 activation has a neurotoxic effect, we then measured the intake of propidium iodide in Wt cerebral cortical neurons 24 h after incubation with either vehicle (control;  $n=8552$  cells) or 5 nM tPA ( $n=2440$  cells). We failed to detect neuronal death in both experimental groups (Fig. 3E;  $P=0.8$ ; two-tailed Student's *t*-test). To determine whether tPA-induced binding of p35 to Cdk5 leads to Cdk5 activation, we examined the expression of protein phosphatase-1 (PP1) phosphorylated at Thr320 (pPP1), a known Cdk5 substrate (Jeanneret et al., 2016; Li et al., 2007), in extracts prepared from Wt cerebral cortical neurons treated for 60 s with 5 nM tPA, alone or in combination with 50  $\mu\text{M}$  roscovitine. Our results show that Cdk5 activation mediates the effect of tPA on PP1 phosphorylation (Fig. 3F,G). Together, these data indicate that tPA

induces p35-mediated Cdk5 activation, and that this effect does not cause neuronal death.

### Effect of tPA on the abundance of p35 in the PSD of NMDA-treated neurons

Because transient exposure to NMDA causes sustained depression of synaptic activity without inducing cell death (Lee et al., 1998), we then decided to use the experimental design described in Fig. 4A to investigate the effect of tPA on the abundance of p35 in the PSD of neurons previously treated with NMDA. We found that incubation for 3 min with 20  $\mu\text{M}$  NMDA, followed 29 min later by treatment for 1 min with either 5 nM tPA or vehicle control, does not induce neuronal death (Fig. 4B). In contrast, our immunocytochemical (Fig. 4C,D) and immunoblotting (Fig. 4E,F) studies show that NMDA treatment decreases the expression of p35 in the PSD, and that this effect is reversed by tPA treatment.

### Cdk5 activation mediates the protective effect of tPA in the PSD

To determine whether tPA-induced p35-mediated Cdk5 activation has an effect on the integrity of the PSD, we used immunocytochemistry and immunoblotting to study the expression of PSD-95 in Wt neurons exposed for 3 min to 20  $\mu\text{M}$  NMDA, followed 29 min later by treatment for 1 min with vehicle (control) or 5 nM tPA, alone or in combination with 50  $\mu\text{M}$  roscovitine, a Cdk5 inhibitor. Our data indicate that incubation with

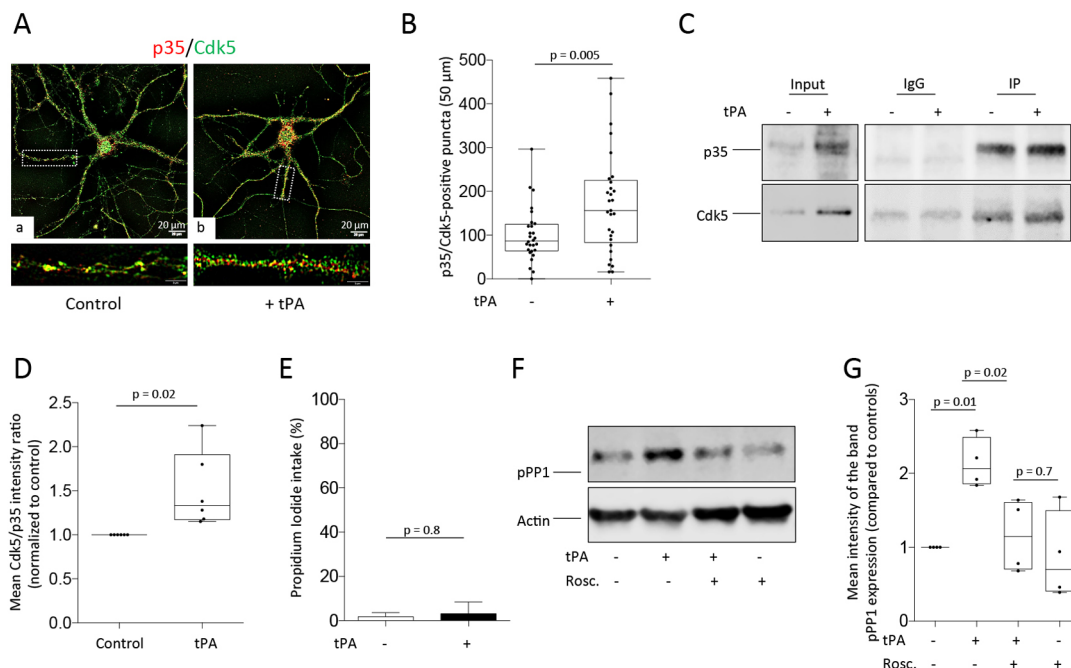


**Fig. 3. tPA induces p35 binding to Cdk5.** (A) Representative confocal microscopy pictures taken at  $60\times$  magnification of p35 (red) and Cdk5 (green) expression in Wt cerebral cortical neurons incubated for 60 s with vehicle (control; a) or 5 nM tPA (b). Lower panels correspond to a  $4\times$  electronic magnification from the regions demarcated by the dashed line boxes in the corresponding panels above. (B) Mean number of p35/Cdk5-positive puncta per 50  $\mu\text{m}$  in extensions from 30 Wt neurons incubated for 60 s with vehicle (control) or 5 nM tPA. Statistical analysis: two-tailed Student's *t*-test. Threshold: 65–255 for red channel and 45–255 for green channel. (C,D) Extracts prepared from Wt cerebral cortical neurons incubated for 60 s with 5 nM tPA or vehicle (control) were immunoprecipitated with anti-p35 antibodies and immunoblotted with antibodies against either Cdk5, p35 or an IgG control (C). D depicts the mean ratio for Cdk5/p35 intensity of the band in six observations per experimental group. Statistical analysis: Student's *t*-test. (E) Mean percentage of cells exhibiting propidium iodide intake following 24 h incubation with vehicle ( $n=8552$  cells) or 5 nM tPA ( $n=2440$  cells). Data are shown as mean  $\pm$  s.d. Statistical analysis: unpaired Student's *t*-test. (F,G) Representative western blot analysis (F) and mean intensity of the band compared to controls (G) in Wt cerebral cortical neurons incubated for 60 s with either vehicle (control) or 5 nM tPA, alone or in the presence of 50  $\mu\text{M}$  roscovitine, or with roscovitine alone.  $n=4$  per experimental conditions. Statistical analysis: two-way ANOVA with Tukey's correction. Scale bars: 20  $\mu\text{m}$  (5  $\mu\text{m}$  in lower panels). For the box plots, the box represents the 25–75th percentiles, and the median is indicated. The whiskers show the complete range. Each dot represents values for individual observations.

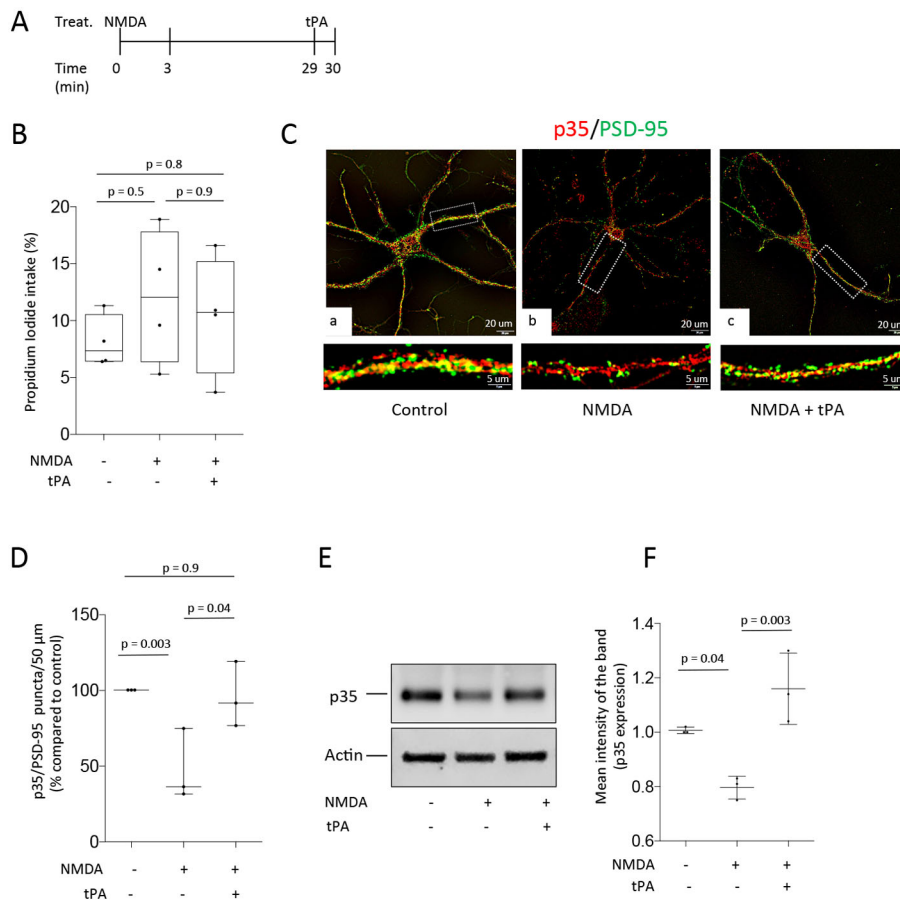


**Fig. 4. tPA reverts the effect of NMDA on the abundance of p35 in the PSD.** (A) Diagram of the experimental design used to study the effect of tPA on p35 expression in neurons previously incubated for 3 min with 20  $\mu$ M NMDA. (B) Mean propidium iodide intake in Wt cerebral cortical neurons kept under physiological conditions ( $n=8315$  cells from four different coverslips), or 24 h after incubation for 3 min with 20  $\mu$ M NMDA, followed by treatment with 5 nM tPA ( $n=7798$  cells from four different coverslips) or vehicle (control;  $n=6275$  cells from four different coverslips). Statistical analysis: one-way ANOVA with Tukey's correction. The box represents the 25–75th percentiles, and the median is indicated. The whiskers show the complete range. Each dot represents values for individual observations. (C) Representative 60 $\times$  confocal microscopy pictures of p35 (red) and PSD-95 (green) expression in Wt cerebral cortical neurons maintained under physiological conditions (a), or incubated for 3 min with 20  $\mu$ M NMDA and then, 29 min later, treated for 1 min with vehicle (control; b) or 5 nM tPA (c). Lower panels correspond to a 4 $\times$  electronic magnification of the areas demarcated by the dashed line boxes in the corresponding panels above. (D) Mean number of p35/PSD-95-positive puncta in 40 extensions from three different groups of Wt neurons exposed to the experimental conditions described in C. Values are given as mean percentage change in the number of p35/PSD-95-positive puncta compared to control cells for each of the three groups of neurons. Threshold: 75–255 for red and green channels. Statistical analysis: one-way ANOVA with Tukey's correction. (E, F) Representative western blot analysis (E) and quantification of the mean intensity of the band (F) of p35 expression in Wt cerebral cortical neurons exposed to the experimental conditions described in panel C.  $n=3$  observations per experimental group. Statistical analysis: one-way ANOVA with Tukey's correction. Scale bars: 20  $\mu$ m (5  $\mu$ m in lower panels).

NMDA decreases the number of PSD-95-positive puncta (Fig. 5A, B) and the expression of PSD-95 in extracts prepared from Wt cerebral cortical neurons (Fig. 5C,D), and that tPA reverses this effect via Cdk5 activation (Fig. 5A–D). To corroborate the observed effect of tPA on the abundance of PSD-95, we studied PSD-95 expression in Wt cerebral cortical neurons incubated with tPA, alone or in the presence of roscovitine. Our data indicate that tPA effectively increases the expression of PSD-95 via Cdk5 activation (Fig. 5E,F).

Because the abundance of PSD-95 in the PSD is regulated by Cdk5 via the ubiquitin-proteasome pathway (Colledge et al., 2003), we then investigated whether tPA has an effect on the ubiquitylation and proteasomal degradation of PSD-95. Extracts prepared from Wt cerebral cortical neurons 15 min after incubating with NMDA for 3 min, followed by treatment with vehicle (control) or tPA, were immunoprecipitated with anti-PSD-95 antibodies and immunoblotted with an antibody against ubiquitin. Our data show that NMDA induces PSD-95 ubiquitylation and that this effect is

attenuated by treatment with tPA (Fig. 5G,H). Because PSD-95 recruits GluR1-containing AMPA receptors to the PSD (Schnell et al., 2002), we then used confocal microscopy to study the colocalization of PSD-95 and GluR1 in the plasma membrane of non-permeabilized Wt cerebral cortical neurons, 30 min after incubating for 3 min with NMDA and treating, 1 min before the end of the experiment, with vehicle (control) or 5 nM tPA. We found that, compared to untreated cells, NMDA-treated cells exhibited a 63.83 $\pm$ 8.9% decrease in the number of PSD-95/GluR1-positive puncta per 50  $\mu$ m ( $P=0.001$ ;  $n=30$  extensions per experimental condition). Remarkably, this effect was reversed by treatment with tPA (26.95 $\pm$ 4.83% decrease in PSD-95/GluR1-positive puncta;  $P=0.02$  compared to cells treated with NMDA without tPA;  $n=30$  cells per experimental group). However, Cdk5 inhibition with roscovitine abrogated the effect of tPA on NMDA-treated cells (62 $\pm$ 9.64% decrease in PSD-95/GluR1-positive puncta;  $P=0.03$  when compared to cells treated with tPA alone; Fig. 5I,J).

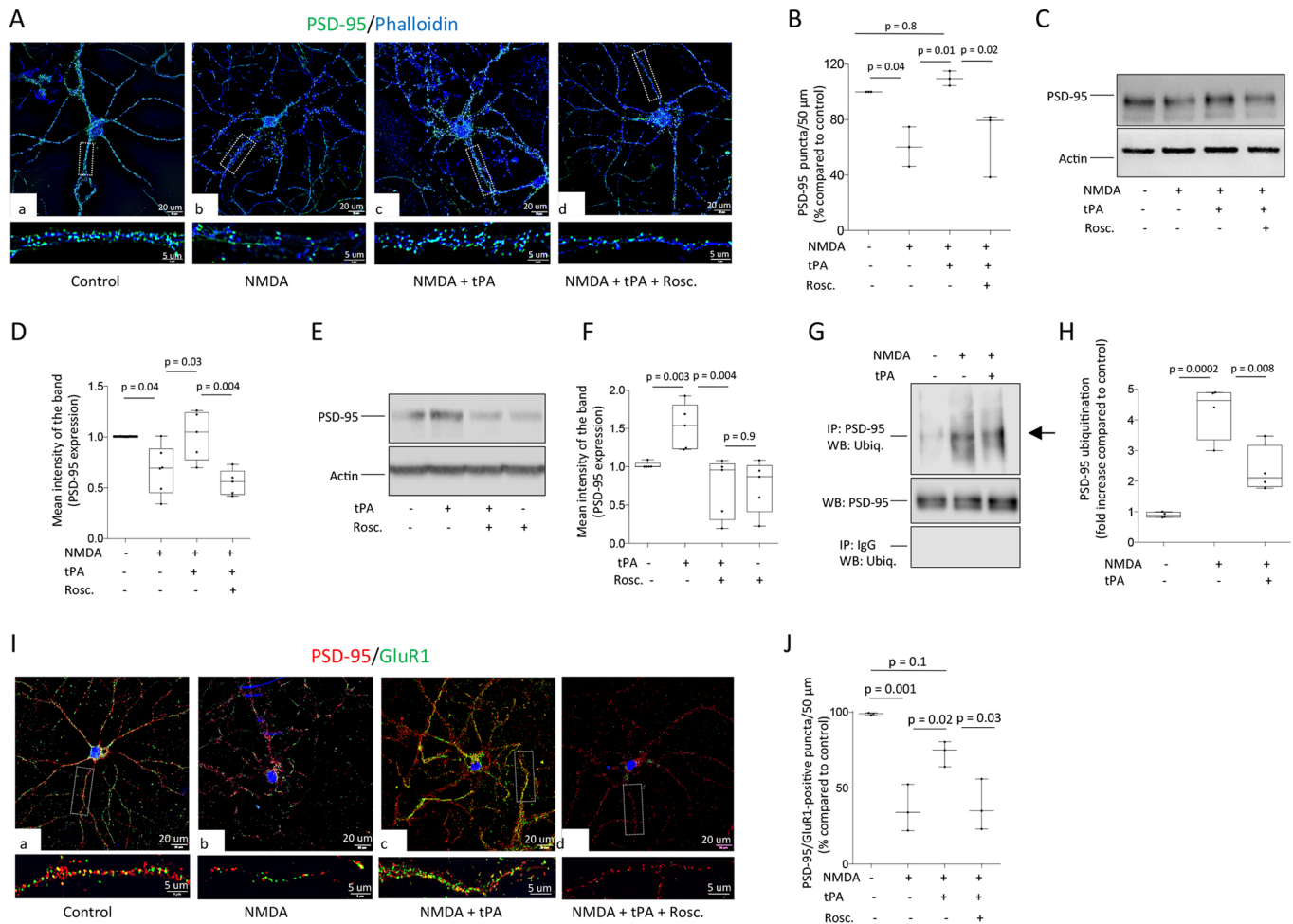


**Fig. 5. tPA reverses the effect of NMDA on PSD-95 expression.** (A) Representative confocal microscopy ( $60\times$  magnification) of PSD-95 (green) and phalloidin (blue) expression in Wt cerebral cortical neurons kept under physiological conditions (a), or incubated for 3 min with  $20\ \mu\text{M}$  NMDA, followed 29 min later by 60 s treatment with either vehicle (control; b) or 5 nM tPA, alone (c) or in the presence of  $50\ \mu\text{M}$  roscovitine (d). Lower panels correspond to a  $4\times$  magnification of the area demarcated by the dashed line boxes in the corresponding panels above. (B) Mean number of PSD-95-positive puncta in 33 extensions from three different groups of Wt neurons exposed to the experimental conditions described in A. Values are given as mean percentage change in the number of p35-positive puncta compared to control cells for each of the three groups of neurons. Threshold: 85–255 for the green channel. Statistical analysis: one-way ANOVA with Tukey's correction. (C,D) Representative western blot analysis (C) and quantification of the mean intensity of the band (D) of PSD-95 expression in Wt cerebral cortical neurons exposed to the experimental conditions described in A.  $n=5$  per experimental condition. Statistical analysis: one-way ANOVA with Tukey's correction. (E,F) Representative western blot analysis of PSD-95 expression in Wt cerebral cortical neurons incubated for 60 s with either vehicle (control) or 5 nM tPA, alone or in the presence of  $50\ \mu\text{M}$  roscovitine, or with roscovitine alone.  $n=5$  observations per experimental condition. Statistical analysis: two-way ANOVA with Tukey's correction. (G) Wt cerebral cortical neurons previously incubated for 3 min with  $20\ \mu\text{M}$  NMDA were treated with 5 nM tPA or a comparable volume of vehicle (control). Fifteen minutes later, cell extracts were immunoprecipitated with an antibody against ubiquitin and immunoblotted with either anti-Cdk5, PSD-95 or IgG antibodies. (H) Mean intensity of the band ( $n=4$  observations per experimental group) of PSD-95 ubiquitination (denoted by the arrow in G) in Wt neurons exposed to the experimental conditions described in G. Statistical analysis: one-way ANOVA with Tukey's correction. (I) Representative confocal microscopy pictures ( $60\times$  magnification) of PSD-95 and GluR1 expression in Wt cerebral cortical neurons exposed to the experimental conditions described in A. Lower panels correspond to a  $4\times$  magnification of the areas demarcated by the dashed line boxes in the corresponding panels above. (J) Mean number of PSD-95/GluR1-positive puncta in 30 extensions from three different groups of Wt neurons exposed to the experimental conditions described in A. Values are given as mean percentage change in the number of PSD-95/GluR1-positive puncta compared to control cells for each of the three groups of neurons. Threshold: 65–255 for the red channel and 35–255 for the green channel. Statistical analysis: one-way ANOVA with Tukey's correction. Scale bars:  $20\ \mu\text{m}$  ( $5\ \mu\text{m}$  in lower panels). For the box plots, the box represents the 25–75th percentiles, and the median is indicated. The whiskers show the complete range. Each dot represents values for individual observations.

## DISCUSSION

The neurovascular unit (NVU) is a highly dynamic system assembled by endothelial cells encased by a basement membrane abutted by astrocytic end-feet processes that in their opposite pole enter in direct contact with synapses from neighboring neurons (Abbott et al., 2006). tPA is abundantly found in each cellular component of the NVU, and its release is pivotal to preserve its structure and function

via plasminogen-dependent and -independent activation of various cell signaling pathways (Yepes et al., 2009). Hence, the release of tPA from endothelial cells into the intravascular space has a fibrinolytic effect mediated by the ability of tPA to catalyze the conversion of plasminogen into plasmin (Collen, 1999); and the release of tPA from perivascular astrocytes into the basement membrane–astrocyte interface regulates the barrier function of the NVU (blood–brain

barrier) by a mechanism that does not require plasmin generation (Polavarapu et al., 2007; Yepes et al., 2003).

A growing body of experimental evidence indicates that tPA also plays a central role in the regulation of synaptic function via plasminogen-dependent and -independent mechanisms. Indeed, synaptic activity induces the rapid expression of tPA (Qian et al., 1993), and its release into the synaptic cleft activates the synaptic vesicle cycle (Wu et al., 2015; Yepes et al., 2016), promotes the synaptic uptake of glucose (Wu et al., 2013, 2012), induces neuroglial coupling (An et al., 2014) and regulates the postsynaptic response to the presynaptic release of glutamate (Jeanneret et al., 2016). In line with these observations, different experimental paradigms have shown that the release of neuronal tPA is pivotal for the development of synaptic plasticity (Baranes et al., 1998).

Recent experimental evidence indicates that the presynaptic release of tPA has a profound effect on the structure and receptor composition of the PSD. Accordingly, tPA induces homeostatic plasticity in cerebral cortical neurons via activation/deactivation of the CaMKII $\alpha$ /PP1 switch in the PSD (Jeanneret et al., 2016), and regulates the expression of PSD-95 by an as yet unknown mechanism (Jeanneret et al., 2018). Here, we report that tPA increases the abundance of p35 in the postsynaptic terminal by preventing its degradation, and that tPA-induced p35-induced Cdk5 activation regulates the receptor composition of the PSD. Our studies indicate that the total amount of p35 in the synapse is the net balance of the local synthesis of proteins and the rapid degradation of membrane-bound p35, and that tPA most likely increases the abundance of p35 by preventing its proteasomal degradation. Remarkably, our data indicate that tPA also prevents the degradation of PSD-95 via Cdk5-mediated inhibition of its ubiquitylation. Further studies are required to determine whether tPA also has an effect on proteasomal-independent degradation pathways, which is suggested by our early studies indicating that tPA activates the mammalian target of rapamycin (mTOR) pathway (Wu et al., 2012). Importantly, we found that the effect of tPA on p35 is mediated by synaptic NMDA receptors, indicating that tPA acts as a bridge between the presynaptic compartment and glutamate receptors anchored to the PSD by PSD-95. We acknowledge that the reported effect of tPA on p35 abundance is very rapid, particularly if it requires the conversion of plasminogen into plasmin. An alternative explanation for our findings is that the increase in p35 abundance is the result of a two-pronged process, in which the non-proteolytic interaction of tPA with an as yet unknown substrate requires the modulatory effect of already formed plasmin on NMDA receptors. This hypothesis is further supported by our early work indicating a modulatory role of plasmin on NMDA receptors in the murine brain (Mannaioni et al., 2008), and a dual, plasmin-dependent and -independent effect of tPA on TrkB (also known as Ntrk2) receptors in the PSD (Jeanneret et al., 2018).

PSD-95 is a member of the membrane-associated guanylate kinase (MAGUK) family of proteins that regulates the anchorage of receptors, ion channels and adhesion molecules to the PSD via their interaction with its PDZ domains (Vallejo et al., 2017). It has been reported that Cdk5 phosphorylates PSD-95 (Morabito et al., 2004), and that Cdk5 inhibition induces the ubiquitylation and proteasomal degradation of PSD-95 (Bianchetta et al., 2011). Here, we show that NMDA not only decreases the expression of p35 in the PSD but also induces PSD-95 ubiquitylation, and that both effects are blocked by tPA. More importantly, we found that tPA prevents NMDA-induced removal of GluR1-containing AMPA receptors from the synapse, which are known to be recruited to the PSD by PSD-95 (Ehrlich and Malinow, 2004). Together, these data indicate that, by its ability to

regulate the degradation of synaptic proteins, tPA modulates the receptor composition of the PSD via Cdk5 activation. Importantly, a link between tPA and Cdk5 is further supported by reports indicating that both Cdk5 (Ye et al., 2014) and tPA (Seeds et al., 1999) are required for neuronal migration in the CNS.

Because it has been proposed that Cdk5 dysregulation promotes cell death and neurodegeneration associated with the cleavage of p35 into p25 (Cheung et al., 2006; Fischer et al., 2005), it is possible to postulate that, by inducing p35 expression and p35-mediated Cdk5 activation, tPA has a neurotoxic effect in the CNS. However, although this hypothesis would agree with a proposed harmful effect of tPA in the brain (Baron et al., 2010), our data indicating that – despite inducing p35-dependent Cdk5 activation – tPA neither promotes cell death nor induces the cleavage of p35 into p25 agrees with previous studies indicating that this protease does not have a neurotoxic effect in the CNS (Echeverry et al., 2010). These observations are in line with studies indicating that Cdk5 activation may also have a neuroprotective effect (Cheung and Ip, 2004), most likely associated with its ability to induce homeostatic plasticity (Seeburg et al., 2008). Here, we used an *in vitro* model of chemical long-term depression to show that depression of synaptic activity leads to a decrease in the abundance of p35 in the PSD, and that this effect is reversed by tPA. More importantly, we show that the harmful effect of NMDA on PSD-95 and GluR1 expression in the PSD is abrogated by tPA-induced Cdk5 activation. In summary, our data indicate a novel role for tPA in the CNS as an inductor of p35-mediated Cdk5 activation, and show that this leads to preservation of the integrity and receptor composition of the PSD.

## MATERIALS AND METHODS

### Animals and reagents

We used neurons cultured from Wt mice (C57BL/6J background) following a protocol approved by the Institutional Animal Care and Use Committee of Emory University, Atlanta, GA. Recombinant murine tPA, proteolytically inactive recombinant tPA [i-tPA; with an alanine for serine substitution at the active site Ser481 (S481A)] and plasmin were acquired from Molecular Innovations (Novi, MI). Other reagents were roscovitine and puromycin (Calbiochem Millipore, Burlington, MA), MK-801, MG-132 and NMDA (Tocris Bioscience, Minneapolis, MN), dynabeads and propidium iodide (Thermo Fisher Scientific, Grand Island, NY), phalloidin-AMCA conjugate (AAT Bioquest, Sunnyvale, CA), and antibodies against PSD-95, p35, ubiquitin, pPP1 and IgG (Cell Signaling Technology, Danvers, MA), Tau (Millipore, Burlington, MA), actin, donkey anti-rabbit Alexa Fluor 488 and donkey anti-mouse Alexa Fluor 494 (Thermo Fisher Scientific), MAP-2 (Sigma-Aldrich, St Louis, MO), Cdk5 (Santa Cruz Biotechnology, Dallas, TX), GluR1 and bassoon (Abcam, Cambridge, MA).

### Neuronal cultures and quantification of cell survival

Cerebral cortical neurons were cultured from embryonic day 16–18 Wt mice as described elsewhere (Echeverry et al., 2010). Briefly, the cerebral cortex was dissected, transferred into Hanks' balanced salt solution containing 100 units/ml penicillin, 100  $\mu$ g/ml streptomycin and 10 mM HEPES, and incubated in trypsin containing 0.02% DNase at 37°C for 15 min. Tissue was triturated and the supernatant was resuspended in GS21-supplemented neurobasal medium containing 2 mM l-glutamine and plated onto 0.1 mg/ml poly-l-lysine-coated wells. Experiments were performed at 16 days *in vitro*. To quantify cell survival, Wt neurons were fixed 24 h after 3 min of incubation with 20  $\mu$ M NMDA followed by treatment with 5 nM tPA or a comparable volume of vehicle (control). The uptake of propidium iodide was studied in each experimental group, following the manufacturer's instructions. Pictures were taken with an Olympus microscope IX83 and a DP80 camera at 10 $\times$  magnification, and propidium iodide-positive neurons per field were automatically counted with the CellSens Dimension software from Olympus. Results are expressed as the percentage of iodide-positive cells following exposure to NMDA in relation to the total number of Hoechst-positive cells.

### Isolation of synaptoneurosomes and PSD-enriched fractions

Wt cerebral cortical neurons were scraped in cold fractionation buffer (1 mM EGTA, 0.25 M sucrose, 25 mM HEPES, pH8.1) in the presence of proteases and phosphatases inhibitors, homogenized using a 5 ml Dounce tissue grinder with ten up-and-down strokes, and centrifuged at 2000 *g* for 5 min to remove cell debris. The supernatant (S1) was transferred to a new tube and centrifuged at 32,000 *g* for 10 min. The pellet (P2) containing synaptoneurosomes was either used for some experiments, or resuspended in 1 ml of a solution containing 150 mM KCl and 0.5% Triton, mixed for 5 min and centrifuged at 275,000 *g* for 1 h. The PSD-containing pellet (P3) was washed again with 0.5 ml of 150 mM KCl and 0.5% Triton buffer, centrifuged at 275,000 *g* for 1 h and lysed in 50 mM Tris-HCl/0.3% SDS buffer for protein assay. To test the purity of these preparations, extracts were immunoblotted with antibodies against PSD-95 (detects the PSD), syntaxin-1 (detects the presynaptic membrane) and synaptophysin (detects synaptic vesicles). Our data indicate that these extracts are highly enriched for PSD-95 but with undetectable levels of both syntaxin-1 and synaptophysin (data not shown).

### Immunoblotting

To study the effect of tPA and plasmin on the abundance of p35, Wt neurons were incubated for 0–60 s with 5 nM proteolytically active tPA, or for 60 s with either 5 nM proteolytically inactive tPA or 100 nM plasmin. To investigate the effect of tPA on the abundance of p35 in the synapse, synaptoneurosomes were prepared from Wt neurons incubated for 60 s with vehicle (control) or 5 nM tPA. To determine the role of NMDA receptors on the effect of tPA on p35, PSD extracts were prepared from Wt neurons treated for 60 s with 5 nM tPA, or with a combination of tPA and 20  $\mu$ M MK-801, or with MK-801 alone. To study the effect of tPA on pPP1, Wt cerebral cortical neurons were incubated for 60 s with 5 nM tPA, alone or in the presence of 50  $\mu$ M roscovitine, or with roscovitine alone. To study the effect of tPA on p35 and PSD-95 expression in cells previously exposed to NMDA, Wt neurons were incubated for 3 min with 20  $\mu$ M NMDA, followed 29 min later by treatment with 5 nM tPA, alone or in the presence of 50  $\mu$ M roscovitine. A subgroup of cells was not incubated with NMDA and instead was treated for 60 s with 5 nM tPA, alone or in the presence of 50  $\mu$ M roscovitine. To study the effect of tPA on the proteasome, Wt neurons were incubated for 15 s with 5 nM tPA or vehicle (control), and then incubated for 30 min with 270  $\mu$ M puromycin. A different group of cells was treated with tPA alone, or with tPA in combination with 100  $\mu$ M of the proteasomal inhibitor MG-132, or with MG-132 alone. In each group of experiments, protein quantification was performed with the BCA assay, and 2.5  $\mu$ g was loaded per sample, separated by 4–20% linear gradient polyacrylamide gel, transferred to a PVDF membrane, blocked with 5% non-fat dry milk in Tris-buffered saline (TBS), pH 7.6, with 0.1% Tween 20 buffer, and incubated with antibodies against either p35 (1:1000) or PSD-95 (1:1000), or pPP1 (1:1000) and  $\beta$ -actin (1:5000). Membranes were developed in a Li-COR Odyssey Imaging System (Lincoln, NE). Densitometry analysis was performed in each band using the Image Studio (Li-COR).

### Immunoprecipitation studies

Lysates prepared from extracts from Wt cerebral cortical neurons treated for 60 s with 5 nM tPA or vehicle (control) were harvested and lysed in RIPA buffer containing proteinase inhibitor and incubated first with 2  $\mu$ g anti-p35 antibodies at 4°C overnight, and then with 500  $\mu$ g Dynabeads Protein G (Life Technologies, Grand Island, NY). Beads were washed five times with 300  $\mu$ l RIPA buffer, immunoprecipitated proteins were eluted with 30  $\mu$ l 2 $\times$  Laemmli Sample Buffer (Bio-Rad, Hercules, CA), boiled for 10 min, and immunoblotted with antibodies against Cdk5 or p35. Results are presented as Cdk5/p35 ratio normalized for controls for each experiment. To study the effect of tPA on NMDA-induced PSD-95 ubiquitylation, Wt cerebral cortical neurons were treated for 3 min with 20  $\mu$ M NMDA followed by incubation with 5 nM tPA or a comparable volume of vehicle (control). Fifteen minutes later, cells were lysed in RIPA buffer, sonicated and centrifuged for 10 min at maximum speed. Then, 500  $\mu$ g of proteins were incubated overnight with 4  $\mu$ g anti-PSD-95 antibodies or IgG (normal), incubated for 1 h with 20  $\mu$ l dynabeads, washed with 1 ml RIPA buffer, and immunoblotted with anti-ubiquitin and anti-PSD-95 antibodies (to ensure

equal loading). Membranes were developed in a Li-COR Odyssey Imaging System and densitometry analysis was performed in each band using the Image Studio (Li-COR).

### Immunohistochemistry

To study the effect of tPA on p35 expression, Wt cerebral cortical neurons were fixed with 4% paraformaldehyde following 60 s of incubation with 5 nM tPA or a comparable volume of vehicle (control). To investigate the effect of tPA on p35, GluR1 and PSD-95 expression in cells previously incubated with NMDA, Wt neurons were fixed 30 min after 3 min of incubation with 20  $\mu$ M NMDA, followed 1 min before the end of the experiment by treatment with 5 nM tPA or vehicle (control), alone or in the presence of 50  $\mu$ M roscovitine. Following fixation, cells were washed three times in TBS and incubated for 30 min in a blocking solution containing 3% bovine serum albumin in TBS. Then, samples were kept overnight in a solution containing anti-p35 (1:100) and either anti-MAP-2 (1:1000), anti-Cdk5 (1:100) or anti-PSD-95 antibodies (1:100); or anti-Tau (1:1000) or anti-bassoon (1:1000) antibodies; or with a combination of anti-PSD-95 antibodies (1:100) and either phalloidin (1:100), anti-GluR1 (1:100) or anti-p35 (1:100) antibodies. To study the colocalization of surface GluR1 with PSD-95, samples were incubated with anti-GluR1 antibodies, permeabilized with 10  $\mu$ g/ml digitonin and then incubated with anti-PSD-95 antibodies. Secondary antibodies were anti-goat Alexa Fluor 488 (1:500) and anti-rabbit Alexa Fluor 594 (1:500). The number of p35/MAP-2-, p35/Cdk5-, p35/PSD-95-, PSD-95/phalloidin- and PSD-95/GluR1-positive puncta was quantified with ImageJ (National Institutes of Health, Bethesda, MD) with the puncta analyzer plugin in pictures taken with a Fluoview FV10i confocal laser-scanning microscope (Olympus) at 60 $\times$  magnification. For quantifications, a 50  $\mu$ m region of interest was drawn over neuronal extensions and a rolling ball background reduction was set up at 15, with threshold for different channels as described in each figure legend. Images were processed using 2D deconvolution with 64 iterations and analyzed with the CellSens Dimension Olympus software. Integrated density of p35 expression in MAP-2 and Tau-positive extensions was measured over each region of interest with the default function of Image J.

### Statistical analysis

Statistical analysis was performed with one- or two-way ANOVA with Tukey's or Dunnett's correction, as indicated in figure legends, or with the Student's *t*-test, as appropriate. *P*<0.05 was considered significant.

### Competing interests

The authors declare no competing or financial interests.

### Author contributions

Conceptualization: A.D., V.J., P. Merino, M.Y.; Methodology: A.D., V.J., P. Merino, M.Y.; Formal analysis: A.D., M.Y.; Investigation: A.D., V.J., P. Merino, P. McCann; Writing - original draft: A.D.; Writing - review & editing: M.Y.; Supervision: M.Y.; Project administration: M.Y.; Funding acquisition: M.Y.

### Funding

This work was supported by the National Heart, Lung, and Blood Institute [NS-091201 to M.Y.], the National Institute of Neurological Disorders and Stroke [NS-079331 to M.Y.] and the U.S. Department of Veterans Affairs [VA Merit Award 101BX003441 to M.Y.]. Deposited in PMC for release after 12 months.

### References

- Abbott, N. J., Rönnbäck, L. and Hansson, E. (2006). Astrocyte-endothelial interactions at the blood-brain barrier. *Nat. Rev. Neurosci.* **7**, 41-53.
- An, J., Haile, W. B., Wu, F., Torre, E. and Yepes, M. (2014). Tissue-type plasminogen activator mediates neuroglial coupling in the central nervous system. *Neuroscience* **257**, 41-48.
- Baranes, D., Lederfein, D., Huang, Y.-Y., Chen, M., Bailey, C. H. and Kandel, E. R. (1998). Tissue plasminogen activator contributes to the late phase of LTP and to synaptic growth in the hippocampal mossy fiber pathway. *Neuron* **21**, 813-825.
- Baron, A., Montagne, A., Cassé, F., Launay, S., Maubert, E., Ali, C. and Vivien, D. (2010). NR2D-containing NMDA receptors mediate tissue plasminogen activator-promoted neuronal excitotoxicity. *Cell Death. Differ.* **17**, 860-871.
- Bianchetta, M. J., Lam, T. T., Jones, S. N. and Morabito, M. A. (2011). Cyclin-dependent kinase 5 regulates PSD-95 ubiquitination in neurons. *J. Neurosci.* **31**, 12029-12035.

- Cheng, D., Hoogenraad, C. C., Rush, J., Ramm, E., Schlager, M. A., Duong, D. M., Xu, P., Wijayawardana, S. R., Hanfelt, J., Nakagawa, T. et al. (2006). Relative and absolute quantification of postsynaptic density proteome isolated from rat forebrain and cerebellum. *Mol. Cell. Proteomics* **5**, 1158-1170.
- Cheung, Z. H. and Ip, N. Y. (2004). Cdk5: mediator of neuronal death and survival. *Neurosci. Lett.* **361**, 47-51.
- Cheung, Z. H., Fu, A. K. Y. and Ip, N. Y. (2006). Synaptic roles of Cdk5: implications in higher cognitive functions and neurodegenerative diseases. *Neuron* **50**, 13-18.
- Colledge, M., Snyder, E. M., Crozier, R. A., Soderling, J. A., Jin, Y., Langeberg, L. K., Lu, H., Bear, M. F. and Scott, J. D. (2003). Ubiquitination regulates PSD-95 degradation and AMPA receptor surface expression. *Neuron* **40**, 595-607.
- Collen, D. (1999). The plasminogen (fibrinolytic) system. *Thromb. Haemost.* **82**, 259-270.
- Dhavan, R. and Tsai, L.-H. (2001). A decade of CDK5. *Nat. Rev. Mol. Cell Biol.* **2**, 749-759.
- Echeverry, R., Wu, J., Haile, W. B., Guzman, J. and Yepes, M. (2010). Tissue-type plasminogen activator is a neuroprotectant in the mouse hippocampus. *J. Clin. Invest.* **120**, 2194-2205.
- Ehrlich, I. and Malinow, R. (2004). Postsynaptic density 95 controls AMPA receptor incorporation during long-term potentiation and experience-driven synaptic plasticity. *J. Neurosci.* **24**, 916-927.
- Fischer, A., Sananbenesi, F., Pang, P. T., Lu, B. and Tsai, L.-H. (2005). Opposing roles of transient and prolonged expression of p25 in synaptic plasticity and hippocampus-dependent memory. *Neuron* **48**, 825-838.
- Floyd, S. R., Porro, E. B., Slepnev, V. I., Ochoa, G.-C., Tsai, L.-H. and De Camilli, P. (2001). Amphiphysin 1 binds the cyclin-dependent kinase (cdk) 5 regulatory subunit p35 and is phosphorylated by cdk5 and cdc2. *J. Biol. Chem.* **276**, 8104-8110.
- Harada, T., Morooka, T., Ogawa, S. and Nishida, E. (2001). ERK induces p35, a neuron-specific activator of Cdk5, through induction of Egr1. *Nat. Cell Biol.* **3**, 453-459.
- Jeanneret, V., Wu, F., Merino, P., Torre, E., Diaz, A., Cheng, L. and Yepes, M. (2016). Tissue-type plasminogen activator (tPA) modulates the postsynaptic response of cerebral cortical neurons to the presynaptic release of glutamate. *Front. Mol. Neurosci.* **9**, 121.
- Jeanneret, V., Ospina, J. P., Diaz, A., Manrique, L. G., Merino, P., Gutierrez, L., Torre, E., Wu, F., Cheng, L. and Yepes, M. (2018). Tissue-type plasminogen activator protects the postsynaptic density in the ischemic brain. *J. Cereb. Blood Flow Metab.* **38**, 1896-1910.
- Lee, H.-K., Kameyama, K., Huganir, R. L. and Bear, M. F. (1998). NMDA induces long-term synaptic depression and dephosphorylation of the GluR1 subunit of AMPA receptors in hippocampus. *Neuron* **21**, 1151-1162.
- Li, T., Chalifour, L. E. and Paudel, H. K. (2007). Phosphorylation of protein phosphatase 1 by cyclin-dependent protein kinase 5 during nerve growth factor-induced PC12 cell differentiation. *J. Biol. Chem.* **282**, 6619-6628.
- Mannaioni, G., Orr, A. G., Hamill, C. E., Yuan, H., Pedone, K. H., McCoy, K. L., Berlinguer Palmieri, R., Junge, C. E., Lee, C. J., Yepes, M. et al. (2008). Plasmin potentiates synaptic N-methyl-D-aspartate receptor function in hippocampal neurons through activation of protease-activated receptor-1. *J. Biol. Chem.* **283**, 20600-20611.
- Matsubara, M., Kusubata, M., Ishiguro, K., Uchida, T., Titani, K. and Taniguchi, H. (1996). Site-specific phosphorylation of synapsin I by mitogen-activated protein kinase and Cdk5 and its effects on physiological functions. *J. Biol. Chem.* **271**, 21108-21113.
- Moncini, S., Lunghi, M., Valmadre, A., Grasso, M., Del Vescovo, V., Riva, P., Denti, M. A. and Venturin, M. (2017). The miR-15/107 family of microRNA genes regulates CDK5R1/p35 with implications for Alzheimer's disease pathogenesis. *Mol. Neurobiol.* **54**, 4329-4342.
- Morabito, M. A., Sheng, M. and Tsai, L. H. (2004). Cyclin-dependent kinase 5 phosphorylates the N-terminal domain of the postsynaptic density protein PSD-95 in neurons. *J. Neurosci.* **24**, 865-876.
- Müller, C. M. and Griesinger, C. B. (1998). Tissue plasminogen activator mediates reverse occlusion plasticity in visual cortex. *Nat. Neurosci.* **1**, 47-53.
- Nicole, O., Docagne, F., Ali, C., Margail, I., Carmeliet, P., MacKenzie, E. T., Vivien, D. and Buisson, A. (2001). The proteolytic activity of tissue-plasminogen activator enhances NMDA receptor-mediated signaling. *Nat. Med.* **7**, 59-64.
- Patrick, G. N., Zhou, P., Kwon, Y. T., Howley, P. M. and Tsai, L.-H. (1998). p35, the neuronal-specific activator of cyclin-dependent kinase 5 (Cdk5) is degraded by the ubiquitin-proteasome pathway. *J. Biol. Chem.* **273**, 24057-24064.
- Pawlak, R., Magarinos, A. M., Melchor, J., McEwen, B. and Strickland, S. (2003). Tissue plasminogen activator in the amygdala is critical for stress-induced anxiety-like behavior. *Nat. Neurosci.* **6**, 168-174.
- Polavarapu, R., Gongora, M. C., Yi, H., Ranganathan, S., Lawrence, D. A., Strickland, D. and Yepes, M. (2007). Tissue-type plasminogen activator-mediated shedding of astrocytic low-density lipoprotein receptor-related protein increases the permeability of the neurovascular unit. *Blood* **109**, 3270-3278.
- Qian, Z., Gilbert, M. E., Colicos, M. A., Kandel, E. R. and Kuhl, D. (1993). Tissue-plasminogen activator is induced as an immediate-early gene during seizure, kindling and long-term potentiation. *Nature* **361**, 453-457.
- Samson, A. L., Nevin, S. T., Croucher, D., Niogo, B., Daniel, P. B., Weiss, T. W., Moreno, E., Monard, D., Lawrence, D. A. and Medcalf, R. L. (2008). Tissue-type plasminogen activator requires a co-receptor to enhance NMDA receptor function. *J. Neurochem.* **107**, 1091-1101.
- Sappino, A. P., Madani, R., Huarte, J., Belin, D., Kiss, J. Z., Wohlwend, A. and Vassalli, J. D. (1993). Extracellular proteolysis in the adult murine brain. *J. Clin. Invest.* **92**, 679-685.
- Schnell, E., Sizemore, M., Karimzadegan, S., Chen, L., Bredt, D. S. and Nicoll, R. A. (2002). Direct interactions between PSD-95 and stargazin control synaptic AMPA receptor number. *Proc. Natl. Acad. Sci. USA* **99**, 13902-13907.
- Seeburg, D. P., Feliu-Mojer, M., Gaiottino, J., Pak, D. T. S. and Sheng, M. (2008). Critical role of CDK5 and Polo-like kinase 2 in homeostatic synaptic plasticity during elevated activity. *Neuron* **58**, 571-583.
- Seeds, N. W., Williams, B. L. and Bickford, P. C. (1995). Tissue plasminogen activator induction in Purkinje neurons after cerebellar motor learning. *Science* **270**, 1992-1994.
- Seeds, N. W., Basham, M. E. and Haffke, S. P. (1999). Neuronal migration is retarded in mice lacking the tissue plasminogen activator gene. *Proc. Natl. Acad. Sci. USA* **96**, 14118-14123.
- Shah, K. and Lahiri, D. K. (2014). Cdk5 activity in the brain-multiple paths of regulation. *J. Cell Sci.* **127**, 2391-2400.
- Takasugi, T., Minegishi, S., Asada, A., Saito, T., Kawahara, H. and Hisanaga, S. (2016). Two degradation pathways of the p35 Cdk5 (Cyclin-dependent Kinase) activation subunit, dependent and independent of ubiquitination. *J. Biol. Chem.* **291**, 4649-4657.
- Tang, D., Chun, A. C., Zhang, M. and Wang, J. H. (1997). Cyclin-dependent kinase 5 (Cdk5) activation domain of neuronal Cdk5 activator. Evidence of the existence of cyclin fold in neuronal Cdk5a activator. *J. Biol. Chem.* **272**, 12318-12327.
- Tomita, S., Nicoll, R. A. and Bredt, D. S. (2001). PDZ protein interactions regulating glutamate receptor function and plasticity. *J. Cell Biol.* **153**, F19-F24.
- Utreras, E., Futatsugi, A., Rudrabhatla, P., Keller, J., Iadarola, M. J., Pant, H. C. and Kulkarni, A. B. (2009). Tumor necrosis factor- $\alpha$  regulates cyclin-dependent kinase 5 activity during pain signaling through transcriptional activation of p35. *J. Biol. Chem.* **284**, 2275-2284.
- Vallejo, D., Codocedo, J. F. and Inestrosa, N. C. (2017). Posttranslational Modifications Regulate the Postsynaptic Localization of PSD-95. *Mol. Neurobiol.* **54**, 1759-1776.
- Wu, F., Wu, J., Nicholson, A. D., Echeverry, R., Haile, W. B., Catano, M., An, J., Lee, A. K., Duong, D., Dammer, E. B. et al. (2012). Tissue-type plasminogen activator regulates the neuronal uptake of glucose in the ischemic brain. *J. Neurosci.* **32**, 9848-9858.
- Wu, F., Nicholson, A. D., Haile, W. B., Torre, E., An, J., Chen, C., Lee, A. K., Duong, D. M., Dammer, E. B., Seyfried, N. T. et al. (2013). Tissue-type plasminogen activator mediates neuronal detection and adaptation to metabolic stress. *J. Cereb. Blood Flow Metab.* **33**, 1761-1769.
- Wu, F., Torre, E., Cuellar-Giraldo, D., Cheng, L., Yi, H., Bichler, E. K., García, P. S. and Yepes, M. (2015). Tissue-type plasminogen activator triggers the synaptic vesicle cycle in cerebral cortical neurons. *J. Cereb. Blood Flow Metab.* **35**, 1966-1976.
- Ye, T., Ip, J. P., Fu, A. K. and Ip, N. Y. (2014). Cdk5-mediated phosphorylation of RapGEF2 controls neuronal migration in the developing cerebral cortex. *Nat. Commun.* **5**, 4826.
- Yepes, M., Sandkvist, M., Moore, E. G., Bugge, T. H., Strickland, D. K. and Lawrence, D. A. (2003). Tissue-type plasminogen activator induces opening of the blood-brain barrier via the LDL receptor-related protein. *J. Clin. Invest.* **112**, 1533-1540.
- Yepes, M., Roussel, B. D., Ali, C. and Vivien, D. (2009). Tissue-type plasminogen activator in the ischemic brain: more than a thrombolytic. *Trends Neurosci.* **32**, 48-55.
- Yepes, M., Wu, F., Torre, E., Cuellar-Giraldo, D., Jia, D. and Cheng, L. (2016). Tissue-type plasminogen activator induces synaptic vesicle endocytosis in cerebral cortical neurons. *Neuroscience* **319**, 69-78.
- Ziff, E. B. (1997). Enlightening the postsynaptic density. *Neuron* **19**, 1163-1174.